Neutrino masses and flavor mixing in a generalized inverse seesaw model with a universal two-zero texture

Ye-Ling Zhou[*]

Institute of High Energy Physics, Chinese Academy of Sciences, Beijing 100049, China
(Received 10 May 2012; published 7 November 2012)

A generalized inverse seesaw model, in which the 9×9 neutrino mass matrix has vanishing (1,1) and (1,3) submatrices, is proposed. This is similar to the universal two-zero texture which gives vanishing (1,1) and (1,3) elements of the 3×3 mass matrices in both the charged lepton and neutrino sectors. We consider the $Z_6 \times Z_6$ group to realize such texture zeros in the framework of the generalized inverse seesaw model. We also analyze the universal two-zero texture in the general case and propose two *Ansätze* to reduce the number of free parameters. Taking account of the new result of θ_{13} from the Daya Bay experiment, we constrain the parameter space of the universal two-zero texture in the general case and in the two *Ansätze*, respectively. We find that one of the *Ansätze* works well.

I. INTRODUCTION

The canonical seesaw mechanism [1] is successful in generating small masses of left-handed neutrinos, but it has no direct experimental testability and encounters a potential hierarchy problem [2]. In the type-I seesaw model with heavy right-handed neutrinos N_R, the left-handed neutrinos ν_L can gain small masses $M_\nu \approx M_D M_R^{-1} M_D^T$ thanks to the huge right-handed neutrino masses M_R. However, to obtain $M_\nu \sim \mathcal{O}(0.1)$ eV, one has to require $M_R \sim \mathcal{O}(10^{14})$ GeV, if M_D is assumed to be at the electroweak scale ($\sim \mathcal{O}(10^2)$ GeV). This makes the right-handed neutrinos far beyond the detectability of any colliders. The hierarchy problem is that a very high seesaw scale will lead to large corrections to the Higgs mass, which makes the Higgs mass of the order of the electroweak scale unnatural. The inverse seesaw model [3] can solve these problems. Moreover, it is possible to predict light sterile neutrinos naturally [4] and provide rich phenomenology such as the nonunitary effect and leptogenesis [5].

The generalized inverse seesaw model (GISM) is an extension of the canonical seesaw mechanism by introducing three right-handed neutrinos N_{Ri} (for $i = 1, 2, 3$), three additional gauge-singlet neutrinos S_{Ri}, and a scalar Φ into the standard model. The Lagrangian in the charged lepton and neutrino sectors [6] is written as

$$-\mathcal{L}_l = \bar{\ell}_L Y_l H E_R + \bar{\ell}_L Y_D \tilde{H} N_R + \bar{N}_R^c Y_S \Phi S_R$$
$$+ \frac{1}{2} \bar{N}_R^c M_R N_R + \frac{1}{2} \bar{S}_R^c M_\mu S_R + \text{H.c.}, \quad (1)$$

in which H, ℓ_L, and E_R stand for the Higgs doublet, three lepton doublets, and three charged-lepton singlets, respectively, in the standard model and $\tilde{H} = i\sigma_2 H^*$. Here Y_l, Y_D, and Y_S are 3×3 Yukawa coupling matrices, and M_R and M_μ are 3×3 symmetric Majorana mass matrices. After spontaneous symmetry breaking (SSB), the scalars acquire their vacuum expectation values (VEVs), and we gain the

[*]zhouyeling@ihep.ac.cn

3×3 charged lepton mass matrix $M_l = Y_l v(H)/\sqrt{2}$ and the 9×9 neutrino mass matrix

$$\mathcal{M} = \begin{pmatrix} \mathbf{0} & M_D & \mathbf{0} \\ M_D^T & M_R & M_S \\ \mathbf{0} & M_S^T & M_\mu \end{pmatrix} \quad (2)$$

in the flavor basis, in which $M_D = Y_D v(H)/\sqrt{2}$ and $M_S = Y_S v(\Phi)/\sqrt{2}$. Here, $v(H)$ and $v(\Phi)$ are the VEVs of H and Φ, respectively. The GISM degrades to the original inverse seesaw model (OISM) when $M_R = \mathbf{0}$ is taken. It can also accommodate a larger range of the sterile neutrino masses than the OISM [4].

If we regard each submatrix of $\mathcal{M}$ in Eq. (2) as a complex number, we turn to a typical pattern of two-zero textures [7]. Different from the models given in Ref. [7], where M_l is chosen to be diagonal and only M_ν has the two-zero texture, we propose the universal two-zero texture (UTZT) [8], in which both M_l and M_ν have two-zero textures. As the similar texture zeros of quark mass matrices can interpret the smallness of flavor-mixing angles in the quark sectors [9], we expect the UTZT will give us a better understanding of the lepton flavor mixing. We write out the charged lepton and left-handed neutrino mass matrices as

$$M_{l,\nu} = \begin{pmatrix} 0 & A_{l,\nu} & 0 \\ A_{l,\nu} & C_{l,\nu} & B_{l,\nu} \\ 0 & B_{l,\nu} & D_{l,\nu} \end{pmatrix}. \quad (3)$$

Some work of this texture has been done in Refs. [10,11]. Generally, texture zeros can be obtained from Abelian symmetries [12]. Later we will see that by means of these symmetries, the two-zero texture of M_l can be directly derived. For the light left-handed neutrino matrix M_ν, if M_D, M_R, M_S, and M_μ all have the two-zero textures, which will be a natural result from the symmetries, the seesaw mechanism can guarantee that M_ν achieves the two-zero texture [8,11].

Recently, the Daya Bay Collaboration reported a relatively large θ_{13} [13] with its best-fit ($\pm 1\sigma$ range) value $\theta_{13} \simeq 8.8° \pm 0.8°$. It is confirmed by the RENO experiment [14]. The experimental results of large θ_{13} give us the following two motivations for the UTZT: (1) Two phenomenological strategies toward understanding lepton flavor mixing are outlined in Ref. [15]. The first one is to start from a nearly constant flavor-mixing pattern, and the second one is to associate the mixing angles with the lepton mass ratios. While it is a nontrivial job to generate a large θ_{13} from the first strategy according to flavor symmetries, one may pay more attention to the second strategy. To implement the second strategy, one generally requires some elements of M_l and M_ν to be zeros or sufficiently small compared with their neighbors, and the two-zero texture is a typical example of this kind. (2) As discussed in Ref. [16], where M_l is diagonal and M_ν has a two-zero texture, it is more likely to obtain a large θ_{13} if M_ν has texture zeros as in Eq. (3) compared with the other texture zeros. Taking advantage of this kind of texture zeros, we expand our discussion to the scenario that both M_l and M_ν have such texture zeros. We expect that such texture can also gain a large θ_{13}.

The rest of this paper is organized as follows. In Sec. II, we propose a model to connect the GISM with the UTZT under the discrete Abelian group $Z_6 \times Z_6$. With this model, we can realize the two-zero textures of M_l, M_D, M_R, M_S, and M_μ. However, the realization of the two-zero texture of M_ν is a little nontrivial. Section III is devoted to seeing how the two-zero texture of M_ν is realized. In Sec. IV, the UTZT is used to explain the lepton flavor mixing, especially for large θ_{13}. Both analytical and numerical results are presented. The predictions for the effective masses in the tritium beta decay and neutrinoless double beta ($0\nu2\beta$) decay are also given in this section. Since the UTZT in the general case has several adjustable parameters, it does not get stringent experimental constraints. In Sec. V, we consider two *Ansätze* of the UTZT to constrain the parameter space. *Ansatz* (A) is a natural approximation based on our model built in Sec. II, and *Ansatz* (B) is a special case which has been considered in Ref. [8]. Section VI is the conclusion of our paper.

II. A MODEL CONNECTING THE UTZT WITH THE GISM

In this section, we illustrate a way to connect the GISM with the UTZT. We rewrite the Lagrangian in the charged lepton and neutrino sectors as

$$
\begin{aligned}
-\mathcal{L}_l = & \bar{\ell}_{Li}(Y_l^a)_{ij}H^a E_{Rj} + \bar{\ell}_{Li}(Y_D^a)_{ij}\tilde{H}^a N_{Rj} \\
& + \bar{N}_{Ri}^c(Y_S^a)_{ij}\Phi^a S_{Rj} + \frac{1}{2}\bar{N}_{Ri}^c(Y_R^a)_{ij}\chi^a N_{Rj} \\
& + \frac{1}{2}\bar{S}_{Ri}^c(Y_\mu^a)_{ij}\phi^a S_{Rj} + \text{H.c.},
\end{aligned} \tag{4}
$$

in which the repeated indices are summed. In our model, we introduce three scalars into each term, so $a = 1, 2, 3$. Comparing Eq. (4) with Eq. (1), we can see that some replacements have been done. Y_lH, $Y_D\tilde{H}$, $Y_S\Phi$ are replaced by $Y_l^a H^a$, $Y_D^a \tilde{H}^a$, $Y_S^a \Phi^a$, respectively, and the scalars χ^a, ϕ^a are introduced to give the Majorana masses of N_R, S_R, respectively. The purpose of doing these replacements has nothing to do with the GISM but is to give the two-zero textures of the mass matrices M_l, M_D, M_S, M_R, and M_μ.

A model for connecting the GISM with the UTZT can be built based on a direct product of groups $G_{1q_1} \times G_{2q_2} \equiv \mathcal{G}$:

(i) Each fermion or scalar transforms under the group G_1 with a charge q_1. This rule aims to realize the GISM. Since it is flavor blind, different flavors in the same multiplet (e.g., N_i and N_j with $i \neq j$) have the same charges q_1, and different scalars in the same Yukawa coupling (e.g., H^a and H^b with $a \neq b$) have the same charges q_1, too.

(ii) Each fermion or scalar transforms under group G_2 with a charge q_2. We choose G_2 to be an Abelian group Z_n to give the UTZT. In this case, different flavors in the same multiplet should have different charges q_2, and different scalars in the same Yukawa coupling term should also have different charges q_2.

Generally speaking, there are many opportunities to choose G_1 and G_2, and it is essentially unnecessary to require that they be equal to each other. Nevertheless, in view of the similar structures of $\mathcal{M}$ and $M_{l,\nu}$, we assume $G_1 = G_2 = Z_n$.

In our model, we choose $n = 6$ and $\mathcal{G} = Z_{6q_1} \times Z_{6q_2}$. The discrete Abelian group Z_6 is given by $Z_6 \equiv \{1, \omega, \omega^2, \omega^3, \omega^4, \omega^5\}$, where $\omega = e^{i\pi/3}$. In Tables I and II we list the charges q_1 and q_2 for each field, respectively. The invariance of the Lagrangian under the $Z_{6q_1} \times Z_{6q_2}$ leads to the following textures of the Yukawa coupling matrices:

$$
Y_A^1 \sim \begin{pmatrix} 0 & \times & 0 \\ \times & 0 & 0 \\ 0 & 0 & \times \end{pmatrix}, \qquad Y_A^2 \sim \begin{pmatrix} 0 & 0 & 0 \\ 0 & 0 & \times \\ 0 & \times & 0 \end{pmatrix},
$$

$$
\text{and} \quad Y_A^3 \sim \begin{pmatrix} 0 & 0 & 0 \\ 0 & \times & 0 \\ 0 & 0 & 0 \end{pmatrix}, \tag{5}
$$

for $Y_A^a = Y_l^a$, Y_D^a, Y_S^a, Y_R^a, and Y_μ^a. After SSB, the scalars gain their VEVs, and we are left with the mass terms

TABLE I.   The charges of the fermions and scalars under Z_{6q_1}.

	$\bar{\ell}_{Li}$	E_{Ri}	N_{Ri}	S_{Ri}	$\tilde{H}^a$	Φ^a	χ^a	ϕ^a
q_1	0	4	2	1	4	3	2	4

TABLE II.   The charges of the fermions and scalars under Z_{6q_2}.

	$\bar{\ell}_{L1}$	$\bar{\ell}_{L2}$	$\bar{\ell}_{L3}$	e_R	μ_R	τ_R	N_{R1}	N_{R2}	N_{R3}	S_{R1}	S_{R2}	S_{R3}
q_2	0	2	1	0	2	1	0	2	1	0	2	1
	$\tilde{H}^1$	$\tilde{H}^2$	$\tilde{H}^3$	Φ^1	Φ^2	Φ^3	χ^1	χ^2	χ^3	ϕ^1	ϕ^2	ϕ^3
q_2	4	3	2	4	3	2	4	3	2	4	3	2

$$-\mathcal{L}_\ell = \bar{E}_L M_l E_R + \bar{\nu}_L M_D N_R + \bar{N}_R^c M_S S_R$$

$$+ \frac{1}{2}\bar{N}_R^c M_R N_R + \frac{1}{2}\bar{S}_R^c M_\mu S_R + \text{H.c.}$$

$$= \bar{E}_L M_l E_R + \frac{1}{2}\overline{(\nu_L \quad N_R^c \quad S_R^c)}\begin{pmatrix} 0 & M_D & 0 \\ M_D^T & M_R & M_S \\ 0 & M_S^T & M_\mu \end{pmatrix}$$

$$\times \begin{pmatrix} \nu_L^c \\ N_R \\ S_R \end{pmatrix} + \text{H.c.}, \tag{6}$$

where M_l, M_D, M_S, M_R, and M_μ are mass matrices originating from the Yukawa coupling matrices and VEVs of the scalars. Taking M_D, for example, we arrive at

$$M_D = \frac{1}{\sqrt{2}}[Y_D^1 v(H^1) + Y_D^2 v(H^2) + Y_D^3 v(H^3)], \tag{7}$$

in which $v(H^a)$ is the VEV of H^a. All the mass matrices M_l, M_D, M_S, M_R, and M_μ have the same two-zero textures as

$$\begin{pmatrix} 0 & \times & 0 \\ \times & \times & \times \\ 0 & \times & \times \end{pmatrix}. \tag{8}$$

In the Appendix, we show that the mass matrix of light left-handed neutrinos is given by a seesawlike formula in the physical region:

$$M_\nu = -M_D(M_R - M_S M_\mu^{-1} M_S^T)^{-1} M_D^T. \tag{9}$$

With this formula, one can prove that M_ν also follows the two-zero texture as in Eq. (8) [11,17]. A detailed analysis will be given in the next section.

We remark that besides Z_6, lots of discrete Abelian groups Z_n can connect the GISM with the UTZT. Even under the same discrete Abelian group, a different arrangement of the charge q_2 may cause different textures of the Yukawa coupling matrices Y_A^1, Y_A^2, and Y_A^3, but it keeps the textures of mass matrices as in Eq. (8) unchanged. In brief, there are many possibilities to link the GISM with the UTZT. However, if one requires that the Abalian discrete symmetry be anomaly free, one must pay attention to the arrangement for the charges q_1 and q_2 of each field to guarantee the anomaly-free conditions [18]. Then, some arrangements for the charges q_1 and q_2 will be ruled out.

III. THE MASS TEXTURE OF ACTIVE NEUTRINOS

We have proposed a way to realize the two-zero textures of M_l, M_D, M_R, M_S, and M_μ. These textures can be obtained immediately from flavor symmetries under the direct product of discrete Abelian groups. However, a realization of the two-zero texture of M_ν is not so obvious. To find its texture, we must turn to the matrices M_D, M_R, M_S, and M_μ, all of which have the same texture zeros. In a way similar to the proof in Refs. [11,17], after giving the two-zero textures of M_D, M_R, M_S, and M_μ, we can prove that the two-zero textures manifest themselves again in M_ν, as a consequence of Eq. (9).

We express each matrix M_a (for $a = D, S, \mu$) as

$$M_a = \begin{pmatrix} 0 & A_a & 0 \\ A_a & C_a & B_a \\ 0 & B_a & D_a \end{pmatrix}. \tag{10}$$

It is easy to find that the inverse matrix of M_μ has another type of texture zeros

$$M_\mu^{-1} = \frac{1}{A_\mu^2 D_\mu}\begin{pmatrix} B_\mu^2 - C_\mu D_\mu & A_\mu D_\mu & -A_\mu B_\mu \\ A_\mu D_\mu & 0 & 0 \\ -A_\mu B_\mu & 0 & A_\mu^2 \end{pmatrix}. \tag{11}$$

Then, using the seesaw formula $M_X \equiv -M_S M_\mu^{-1} M_S^T$, we find M_X has the two-zero texture as

$$M_X = \begin{pmatrix} 0 & A_X & 0 \\ A_X & C_X & B_X \\ 0 & B_X & D_X \end{pmatrix} \tag{12}$$

with

$$A_X = -\frac{A_S^2}{A_\mu},$$

$$B_X = -\frac{A_S B_S}{A_\mu} + \frac{A_S B_\mu D_S}{A_\mu D_\mu} - \frac{B_S D_S}{D_\mu},$$

$$C_X = -\frac{2A_S C_S}{A_\mu} + \frac{A_S^2 C_\mu}{A_\mu^2} - \frac{(A_\mu B_S - A_S B_\mu)^2}{A_\mu^2 D_\mu}, \tag{13}$$

$$D_X = -\frac{D_S^2}{D_\mu}.$$

Thus, the two-zero texture is invariant under the seesaw transformation.

Repeating the above process for $M_\nu = -M_D(M_R + M_X)^{-1} M_D^T$, we finally obtain that M_ν has the two-zero texture as in Eq. (3). The nonzero entries are given by

$$A_\nu = -\frac{A_D^2}{A_R + A_X},$$

$$B_\nu = -\frac{A_D B_D}{A_R + A_X} + \frac{A_D(B_R + B_X)D_D}{(A_R + A_X)(D_R + D_X)} - \frac{B_D D_D}{D_R + D_X},$$

$$C_\nu = -\frac{2A_D C_D}{A_R + A_X} + \frac{A_D^2(C_R + C_X)}{(A_R + A_X)^2}$$
$$- \frac{[(A_R + A_X)B_D - A_D(B_R + B_X)]^2}{(A_R + A_X)^2(D_R + D_X)},$$

$$D_\nu = -\frac{D_D^2}{D_R + D_X}. \tag{14}$$

It is an exact consequence of the GISM and two-zero textures of M_D, M_R, M_S, and M_μ.

All the 3×3 mass matrices M_l, M_ν, M_D, M_R, M_S, and M_μ have parallel structures with each other. And they are all fractally similar to the 9×9 GISM neutrino matrix $\mathcal{M}$. These similarities can be guaranteed in the framework of flavor symmetries.

IV. FLAVOR MIXING IN THE UTZT

In this section we analyze the flavor mixing in the general UTZT case. The renormalization-group effect might in general modify the two-zero textures of M_l and M_ν, but it is negligibly small in the inverse seesaw model [19] because the TeV seesaw scale is so close to the electroweak scale. Hence, we just discuss the UTZT at the electroweak scale.

The charged lepton and left-handed neutrino mass matrices with two-zero textures have been given in Eq. (3), where $A_{l,\nu}$, $B_{l,\nu}$, $C_{l,\nu}$, and $D_{l,\nu}$ are complex numbers. Some works on this texture have been done in Refs. [8,10], but a general analysis has been lacking in the literature.

As a symmetric matrix, M_l can be diagonalized as $M_l = V_l \hat{M}_l V_l^T$. Here, $\hat{M}_l = \mathrm{Diag}\{m_e, m_\mu, m_\tau\}$, $V_l = Q_l U_l P_l$, $Q_l = \mathrm{Diag}\{e^{i\alpha_l}, e^{i\beta_l}, 1\}$, $P_l = \mathrm{Diag}\{e^{i\gamma_e}, e^{i\gamma_\mu}, e^{i\gamma_\tau}\}$, and U_l is given by

$$U_l = \begin{pmatrix} 1 & 0 & 0 \\ 0 & c_e & s_e \\ 0 & -s_e & c_e \end{pmatrix} \begin{pmatrix} c_\mu & 0 & \hat{s}_\mu^* \\ 0 & 1 & 0 \\ -\hat{s}_\mu & 0 & c_\mu \end{pmatrix}$$
$$\times \begin{pmatrix} c_\tau & s_\tau & 0 \\ -s_\tau & c_\tau & 0 \\ 0 & 0 & 1 \end{pmatrix}, \tag{15}$$

in which $c_\alpha = \cos\theta_\alpha$, $s_\alpha = \sin\theta_\alpha$ (for $\alpha = e$, μ, τ), and $\hat{s}_\mu = s_\mu e^{i\delta_\mu}$.

Similarly, M_ν can be diagonalized as $M_\nu = V_\nu \hat{M}_\nu V_\nu^T$. Here, $\hat{M}_\nu = \mathrm{Diag}\{m_1, m_2, m_3\}$, $V_\nu = Q_\nu U_\nu P_\nu$, $Q_\nu = \mathrm{Diag}\{e^{i\alpha_\nu}, e^{i\beta_\nu}, 1\}$, and $P_\nu = \mathrm{Diag}\{e^{i\gamma_1}, e^{i\gamma_2}, e^{i\gamma_3}\}$, and U_ν is given by

$$U_\nu = \begin{pmatrix} 1 & 0 & 0 \\ 0 & c_1 & s_1 \\ 0 & -s_1 & c_1 \end{pmatrix} \begin{pmatrix} c_2 & 0 & \hat{s}_2^* \\ 0 & 1 & 0 \\ -\hat{s}_2 & 0 & c_2 \end{pmatrix} \begin{pmatrix} c_3 & s_3 & 0 \\ -s_3 & c_3 & 0 \\ 0 & 0 & 1 \end{pmatrix}, \tag{16}$$

in which $c_i = \cos\theta_i$, $s_i = \sin\theta_i$ (for $i = 1$, 2, 3), and $\hat{s}_2 = s_2 e^{i\delta_2}$.

The Maki-Nakagawa-Sakata-Pontecorvo (MNSP) matrix [20] is defined by $V \equiv V_l^\dagger V_\nu = P_l^\dagger U_l^\dagger \bar{Q} U_\nu P_\nu$, in which $\bar{Q} = \mathrm{Diag}\{e^{i\alpha}, e^{i\beta}, 1\}$ and α, β are two combined parameters defined as $\alpha \equiv \alpha_\nu - \alpha_l$, $\beta \equiv \beta_\nu - \beta_l$, respectively. V can be parametrized as $V = QUP$. Here,

$$U = \begin{pmatrix} 1 & 0 & 0 \\ 0 & c_{23} & s_{23} \\ 0 & -s_{23} & c_{23} \end{pmatrix} \begin{pmatrix} c_{13} & 0 & \hat{s}_{13}^* \\ 0 & 1 & 0 \\ -\hat{s}_{13} & 0 & c_{13} \end{pmatrix}$$
$$\times \begin{pmatrix} c_{12} & s_{12} & 0 \\ -s_{12} & c_{12} & 0 \\ 0 & 0 & 1 \end{pmatrix}, \tag{17}$$

in which $c_{ij} = \cos\theta_{ij}$, $s_{ij} = \sin\theta_{ij}$ (for $ij = 12$, 23, 13), and $\hat{s}_{13} = s_{13} e^{i\delta}$. P and Q are two diagonal phase matrices. As the charged leptons are the Dirac fermions, Q is unphysical and can be rotated away by the phase redefinition of the charged lepton fields. But for the Majorana neutrinos, only one overall phase in P can be rotated away, and the other two phases are physical. In this case, P can be parametrized as $P = \mathrm{Diag}\{e^{i\rho}, e^{i\sigma}, 1\}$.

A. Charged leptons

Here, we derive some relations of the mixing parameters in the charged lepton sector. Since the (1,1) and (1,3) elements of M_l are equal to zeros, we obtain

$$\frac{m_e e^{2i\gamma_e}}{m_\tau e^{2i\gamma_\tau}} = -\frac{\hat{s}_\mu^*}{c_\mu^2}\left(\frac{c_e s_\tau}{s_e c_\tau} + \hat{s}_\mu^*\right),$$
$$\frac{m_\mu e^{2i\gamma_\mu}}{m_\tau e^{2i\gamma_\tau}} = +\frac{\hat{s}_\mu^*}{c_\mu^2}\left(\frac{c_e c_\tau}{s_e s_\tau} - \hat{s}_\mu^*\right). \tag{18}$$

A straightforward calculation leads us to the relations of the angles

$$\cot^2\theta_e = s_\mu^2\left(\sqrt{x_l^2 y_l^2\cot^4\theta_\mu - \sin^2\delta_\mu} - \cos\delta_\mu\right)$$
$$\times\left(\sqrt{y_l^2\cot^4\theta_\mu - \sin^2\delta_\mu} + \cos\delta_\mu\right),$$

$$\tan^2\theta_\tau = \frac{\sqrt{x_l^2 y_l^2\cot^4\theta_\mu - \sin^2\delta_\mu} - \cos\delta_\mu}{\sqrt{y_l^2\cot^4\theta_\mu - \sin^2\delta_\mu} + \cos\delta_\mu}, \tag{19}$$

and those of the phases

$$\tan(2\gamma_e - 2\gamma_\tau + \delta_\mu) = \frac{\sin\delta_\mu}{\sqrt{x_l^2 y_l^2\cot^4\theta_\mu - \sin^2\delta_\mu}}, \tag{20}$$

$$\gamma_\mu - \gamma_\tau + \delta_\mu/2 = 0,$$

where $x_l = m_e/m_\mu$ and $y_l = m_\mu/m_\tau$. Taking $m_e = 0.486$ MeV, $m_\mu = 102.7$ MeV, and $m_\tau = 1746$ MeV at the electroweak scale [21] as inputs, we get $x_l = 0.0047$ and $y_l = 0.059$. To assure that Eq. (19) has a real and positive solution, we require

$$0 \leq \theta_\mu \leq \arctan\sqrt{x_l y_l} \approx 1°,$$
$$0 \leq \theta_\tau \leq \arctan\sqrt{2x_l} \approx 6°, \tag{21}$$
$$0 \leq \theta_e \leq 90°.$$

In particular, $\theta_\tau \approx \arctan\sqrt{x_l} \approx 4°$ for $\delta_\mu = \pm 90°$, $0 \leq \theta_\tau < 4°$ for $|\delta_\mu| < 90°$, and $4° \leq \theta_\tau \leq 6°$ for $|\delta_\mu| \geq 90°$. Due to the large mass hierarchy of the charged leptons, θ_μ and θ_τ are very small. They can be regarded as the corrections to the MNSP matrix. Suppressed by s_μ, the phase δ_μ has little influence in the MNSP matrix. Particularly, we have three special cases:

(1) $\tan\theta_e \ll 1/\sqrt{y_l}$,

$$\tan\theta_\mu \approx \sqrt{x_l y_l} \tan\theta_e,$$
$$\tan\theta_\tau \approx \sqrt{x_l}, \tag{22}$$
$$\gamma_e \approx \gamma_\mu \pm 90°,$$

(2) $\tan\theta_e \gg 1/\sqrt{y_l}$,

$$\tan\theta_\mu \approx \sqrt{x_l y_l},$$
$$\tan\theta_\tau \approx \sqrt{\frac{x_l}{y_l}}\cot\theta_e, \tag{23}$$
$$\gamma_e \approx \gamma_\mu - \delta_\mu/2 \pm 90°,$$

and
(3) $\tan\theta_e \sim \mathcal{O}(1/\sqrt{y_l})$,

where one can find $\tan\theta_\mu \sim \mathcal{O}(\sqrt{x_l y_l})$ and $\tan\theta_\tau \sim \mathcal{O}(\sqrt{x_l})$ from Eq. (19). In the leading-order approximation of s_μ and s_τ, we obtain

$$s_\mu^2 \approx \frac{-x_l y_l^2 \cos(\gamma_e - \gamma_\mu)}{x_l + y_l \tan^2\theta_e},$$
$$s_\tau^2 \approx \frac{-x_l \cos(\gamma_e - \gamma_\mu)}{x_l + y_l \tan^2\theta_e}, \tag{24}$$
$$\sin\delta_\mu \approx x_l y_l \sin(\theta_e - \theta_\mu),$$

and $\gamma_e - \gamma_\mu$ is arbitrary.

B. Neutrinos

For the left-handed neutrinos, since the (1,1) and (1,3) elements of M_ν equal zeros, we obtain

$$\frac{m_1 e^{2i\gamma_1}}{m_3 e^{2i\gamma_3}} = -\frac{\hat{s}_2^*}{c_2^2}\left(\frac{c_1 s_3}{s_1 c_3} + \hat{s}_2^*\right),$$
$$\frac{m_2 e^{2i\gamma_2}}{m_3 e^{2i\gamma_3}} = +\frac{\hat{s}_2^*}{c_2^2}\left(\frac{c_1 c_3}{s_1 s_3} - \hat{s}_2^*\right). \tag{25}$$

Later in the numerical calculations, we will see that θ_2 is a small angle, in the same order of magnitude as θ_{13}. In this case, we find $m_1 < m_3$ from Eq. (25). Only the normal hierarchy of neutrino masses is possible in this texture. A straightforward calculation leads us to the relations of the angles

$$\cot^2\theta_1 = s_2^2\left(\sqrt{x_\nu^2 y_\nu^2 \cot^4\theta_2 - \sin^2\delta_2} - \cos\delta_2\right)$$
$$\times \left(\sqrt{y_\nu^2 \cot^4\theta_2 - \sin^2\delta_2} + \cos\delta_2\right),$$
$$\tan^2\theta_3 = \frac{\sqrt{x_\nu^2 y_\nu^2 \cot^4\theta_2 - \sin^2\delta_2} - \cos\delta_2}{\sqrt{y_\nu^2 \cot^4\theta_2 - \sin^2\delta_2} + \cos\delta_2}, \tag{26}$$

and those of the phases

$$\tan(2\gamma_1 - 2\gamma_3 + \delta_2) = \frac{\sin\delta_2}{\sqrt{x_\nu^2 y_\nu^2 \cot^4\theta_2 - \sin^2\delta_2}},$$
$$\tan(2\gamma_2 - 2\gamma_3 + \delta_2) = \frac{-\sin\delta_2}{\sqrt{y_\nu^2 \cot^4\theta_2 - \sin^2\delta_2}}, \tag{27}$$

in which $x_\nu = m_1/m_2$, $y_\nu = m_2/m_3$ and $x_\nu, y_\nu < 1$. To make Eq. (26) have a real and positive solution, we require

$$0 \leq \theta_2 \leq \arctan\sqrt{x_\nu y_\nu},$$
$$0 \leq \theta_3 \leq \arctan\sqrt{2x_\nu}, \tag{28}$$
$$0 \leq \theta_1 \leq 90°.$$

C. The MNSP matrix

We have obtained some relations of the mixing parameters in both the charged lepton and left-handed neutrino sectors. Using these parameters, we can calculate the mixing angles in the MNSP matrix and some other physical observables. And using the experimental constraints, we may find the allowed ranges of the parameters and make predictions for the observables.

The MNSP matrix V can be calculated through $V = V_l^\dagger V_\nu$. Considering the smallness of s_μ, s_τ, and s_2, we obtain the approximate expressions of the mixing angles θ_{13}, θ_{12}, and θ_{23}:

$$\sin\theta_{13} \approx |\hat{s}_2^* e^{i\alpha} + c_1(s_e s_\tau - c_e \hat{s}_\mu^*) - s_1(c_e s_\tau + s_e \hat{s}_\mu^*)e^{i\beta}|,$$
$$\tan\theta_{12} \approx \left|\tan\theta_3 - \frac{e^{-i\alpha}}{c_3^2}[c_1(c_e s_\tau + s_e \hat{s}_\mu^*)e^{i\beta}\right.$$
$$\left. + s_1(s_e s_\tau - c_e \hat{s}_\mu^*)]\right|,$$
$$\sin\theta_{23} \approx |c_e s_1 e^{i\beta} - c_1 s_e|. \tag{29}$$

These expressions hold to the first order in s_μ, s_τ, and s_2. We make some comments on the formulas of the mixing angles in Eq. (29):

(i) Note that θ_{13} is in the same order of magnitude as θ_2, and $\theta_2 \lesssim \arctan\sqrt{x_\nu y_\nu} = \arctan\sqrt{m_1/m_3}$. To generate a relatively large θ_{13}, m_1 cannot be too small.

(ii) Since θ_μ and θ_τ are small, $\theta_{12} \approx \theta_3$ holds. The two-zero texture in the charged lepton sector just has a small contribution to θ_{12}.

(iii) θ_{23} is an overall result of θ_1, θ_e, and β. The two-zero textures in both the charged lepton and neutrino sectors may have large contributions to θ_{23}.

We conclude that except for θ_{12}, both θ_{13} and θ_{23} may receive relatively large corrections from the charged lepton sector. This is one of the features that make the UTZT different from the texture zeros discussed in Ref. [7], in which M_l is diagonal and only M_ν has texture zeros.

The strength of CP violation in the neutrino oscillation experiments is measured by the Jarlskog invariant $\mathcal{J} = \mathrm{Im}(V_{e1}V_{\mu2}V_{e2}^*V_{\mu1}^*) = c_{12}s_{12}c_{23}s_{23}c_{13}^2s_{13}\sin\delta$ [22]. For current experimental data of θ_{13}, one may expect a relatively large $\mathcal{J}$ if the CP-violating phase δ is not suppressed. In the leading-order approximation of s_μ, s_τ, and s_2,

$$\mathcal{J} \approx s_\mu J_\mu + s_\tau J_\tau + s_2 J_2, \tag{30}$$

in which

$$J_\mu = -s_3 c_3 [s_1 c_e \sin(\alpha + \delta_\mu) - c_1 s_e \sin(\alpha + \delta_\mu - \beta)]$$
$$\times (c_1^2 c_e^2 + s_1^2 s_e^2 + 2c_1 s_1 c_e s_e \cos\beta),$$
$$J_\tau = -s_3 c_3 [s_1 s_e \sin\alpha + c_1 c_e \sin(\alpha - \beta)]$$
$$\times (c_1^2 s_e^2 + s_1^2 c_e^2 - 2c_1 s_1 c_e s_e \cos\beta),$$
$$J_2 = s_3 c_3 (c_e s_e \sin\beta \cos\delta_2 + c_1 s_1 \sin\delta_2 \cos2\theta_e$$
$$- c_e s_e \cos\beta \sin\delta_2 \cos2\theta_1). \tag{31}$$

One can see that the first term $s_\mu J_\mu$ is in general the smallest one because of the smallness of s_μ, and the last two terms $s_\tau J_\tau$ and $s_2 J_2$ may have comparable contributions to $\mathcal{J}$.

The $0\nu2\beta$ decay experiments are important for examining if neutrinos are the Majorana fermions. One key parameter in such experiments is the effective mass $\langle m \rangle_{ee} \equiv (V\hat{M}_\nu V^T)_{11} = (V_l^\dagger M_\nu V_l^*)_{11}$. The pattern in which M_ν has the two-zero texture in Eq. (8) and M_l is diagonal gives $\langle m \rangle_{ee} = 0$. Different from such a pattern, the 0UTZT that we are considering here yields a nonzero $\langle m \rangle_{ee}$. In the leading-order approximation of s_μ, s_τ, and s_2, $\langle m \rangle_{ee}$ reads

$$\langle m \rangle_{ee} \approx 2|(U_l)_{21}^*(M_\nu)_{21}| \approx 2|c_e s_\tau + s_e \hat{s}_\mu||A_\nu|, \tag{32}$$

in which

$$|A_\nu| \approx |m_3 s_1 s_2^* e^{2i\gamma_3} - m_1 c_1 c_3 s_3 e^{2i\gamma_1} + m_2 c_1 c_3 s_3 e^{2i\gamma_2}|. \tag{33}$$

In comparison, the effective mass $\langle m \rangle_e$ in the tritium beta decay is given by

$$\langle m \rangle_e \equiv \sqrt{(V\hat{M}_\nu^2 V^\dagger)_{11}} \approx |A_\nu|. \tag{34}$$

Then, we arrive at

$$\frac{\langle m \rangle_{ee}}{\langle m \rangle_e} \approx 2|c_e s_\tau + s_e \hat{s}_\mu|. \tag{35}$$

If we assume $\theta_\tau = 4°$ and ignore the smallness of θ_μ, then we obtain $\langle m \rangle_{ee}/\langle m \rangle_e \simeq 0.1$.

D. Numerical results

In the numerical calculations, we choose seven free parameters θ_e, θ_2, δ_μ, δ_2, α, β, and m_1 as inputs. The values of the charged lepton masses have been given in Sec. IV B. To be compatible with the experimental results, we choose $\Delta m_{21}^2 \simeq (7.4 - 7.8) \times 10^{-5}$ eV^2, $\Delta m_{31}^2 \simeq (2.4 - 2.7) \times 10^{-3}$ eV^2, $\theta_{23} \simeq (42°-49°)$, $\theta_{12} \simeq (33°-35°)$ and the new data $\theta_{13} \simeq (8.0°-9.6°)$ from the Daya Bay experiment as constraints. With the help of these data, we can obtain the allowed ranges of the input parameters and calculate the observables.

In Fig. 1, we show the comparison of the values between θ_1 and θ_e and that of the values between θ_2 and θ_τ. The first two angles are dominant parameters in the expression of θ_{23}, while the last two angles are dominant parameters in the expression of θ_{13} [see Eq. (29)]. Numerically, we obtain $\theta_1 \simeq (24°-72°)$ versus $\theta_e \simeq (0-90°)$ for θ_{23}, and $\theta_2 \simeq (4°-13°)$ versus $\theta_\tau \simeq (0-6°)$ for θ_{13}. A lot of points are located around $\theta_\tau = 4°$, indicating that $\delta_\mu \approx \pm90°$ is favored.

In Fig. 2, we show the parameter space and some phenomenological predictions in the general case. We plot the allowed regions of (θ_{13}, m_1) and $(\theta_{12}, \theta_{23})$ parameters first
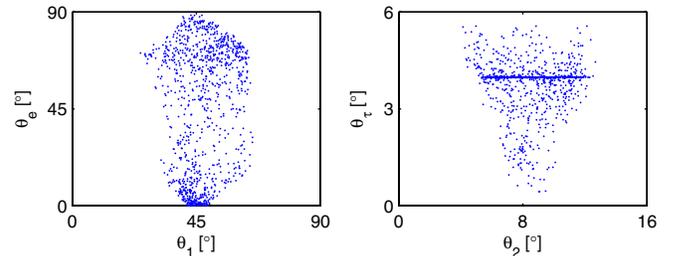
FIG. 1 (color online). The comparison of the values between θ_1 and θ_e (left) and that of the values between θ_2 and θ_τ (right). The free parameters θ_e, θ_3, δ_μ, δ_2, α, β, and m_1 are used as inputs. The constraints are given by $\Delta m_{21}^2 \simeq (7.4-7.8) \times 10^{-5}$ eV^2, $\Delta m_{31}^2 \simeq (2.4-2.7) \times 10^{-3}$ eV^2, $\theta_{23} \simeq (42°-49°)$, $\theta_{12} \simeq (33°-35°)$, and $\theta_{13} \simeq (8.0°-9.6°)$.
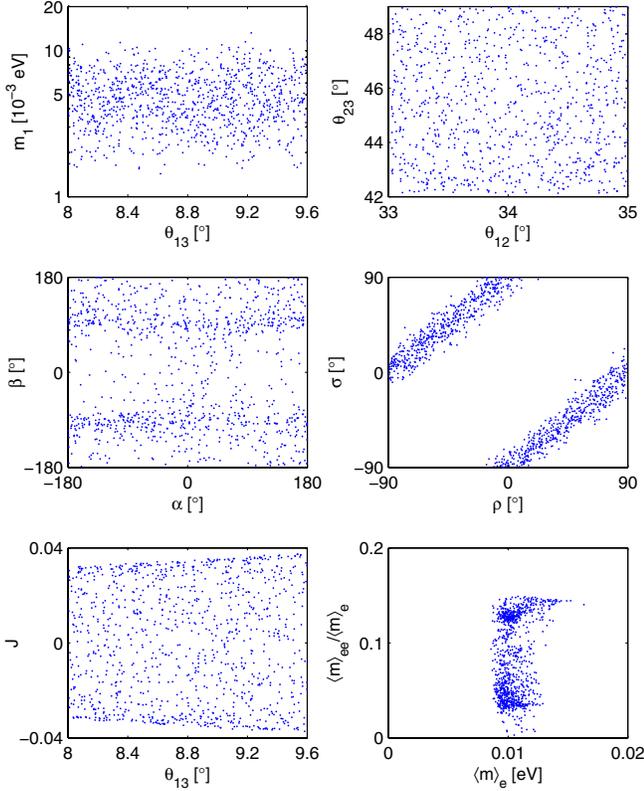
FIG. 2 (color online). The parameter space and phenomenological predictions in the general case. The inputs and constraints are the same as in Fig. 1.

in the figure. The lightest neutrino mass m_1 is constrained in the range (0.001–0.015) eV. The points of the mixing angles θ_{12}, θ_{23}, and θ_{13} are nearly evenly distributed in the full parameter space. Predictions for parameters related to *CP* violation are shown then. There is little restriction on the combined input parameters α and β except that β is more likely to approach $\pm 90°$. For the Majorana phases ρ and σ, the relation $\rho \simeq \sigma \pm 90°$ holds roughly. The numerical result of the Jarlskog invariant $\mathcal{J}$ is also shown in Fig. 2. Due to the largeness of θ_{13}, $|\mathcal{J}|$ can reach several percent. Concretely, it can maximally reach 0.03 at $\theta_{13} = 8°$ and 0.04 at $\theta_{13} = 9.6°$. The effective masses in the tritium beta decay and $0\nu 2\beta$ decay are shown at the end of Fig. 2. One can see that the ratio $\langle m \rangle_{ee} / \langle m \rangle_e$ is of $\mathcal{O}(0.1)$ in most cases. Since $\langle m \rangle_e \simeq 0.01$ eV is referred in Fig. 2, $\langle m \rangle_{ee}$ can maximally reach 10^{-3} eV. However, this is still below the sensitivity of the near-future experiments, which is expected to be $\langle m \rangle_{ee} \simeq (1 - 5) \times 10^{-2}$ eV [23].

One can reconstruct the charged lepton and left-handed neutrino mass matrices with the help of the experimental constraints. Considering that there are cancellations in some special cases, leading to vanishing values of $A_{l,\nu}$, $B_{l,\nu}$, $C_{l,\nu}$ or $D_{l,\nu}$, the positive lower bounds may not exist. But one can expect that there are some ranges in which most of the points are located. In our calculation, we find that 95% of the points are located in the following ranges:

$$|A_l| \simeq (7.4 - 31) \text{ MeV}, \qquad |B_l| \simeq (0.046 - 0.94) \text{ GeV},$$
$$|C_l| \simeq (0.96 - 1.8) \text{ GeV}, \qquad |D_l| \simeq (0.11 - 1.8) \text{ GeV},$$
$$\tag{36}$$

and

$$|A_\nu| \simeq (0.0073 - 0.018) \text{ eV}, \qquad |B_\nu| \simeq (0.019 - 0.028) \text{ eV},$$
$$|C_\nu| \simeq (0.011 - 0.040) \text{ eV}, \qquad |D_\nu| \simeq (0.010 - 0.048) \text{ eV}.$$
$$\tag{37}$$

In the neutrino sector, all the elements of M_ν are in the $\mathcal{O}(0.01)$ eV order. But in the charged lepton sector, the elements of M_l vary within some wide ranges because of the uncertainty of θ_e.

V. LARGE θ_{13} AND TWO *ANSÄTZE* OF THE UTZT

In the previous section, we have considered the UTZT in the general case. Since there are seven free parameters as inputs, it does not get stringent experimental constraints. We shall consider some special cases of the UTZT to simplify its texture.

First, we assume that the condition [8]

$$\arg(C_{l,\nu}) + \arg(D_{l,\nu}) = 2 \arg(B_{l,\nu}) \tag{38}$$

is satisfied. Then M_l and M_ν are, respectively, decomposed into

$$M_l = P_l^T \bar{M}_l P_l e^{2i\gamma_\tau} \quad \text{and} \quad M_\nu = P_\nu^T \bar{M}_\nu P_\nu e^{2i\gamma_3}, \tag{39}$$

in which

$$\bar{M}_{l,\nu} = \begin{pmatrix} 0 & |A_{l,\nu}| & 0 \\ |A_{l,\nu}| & |C_{l,\nu}| & |B_{l,\nu}| \\ 0 & |B_{l,\nu}| & |D_{l,\nu}| \end{pmatrix}. \tag{40}$$

In the following discussions, we turn to two different *Ansätze*: *Ansatz* (A), $|A_{l,\nu}| = |D_{l,\nu}|$ and *Ansatz* (B), $|C_l| = |B_l|$ and $|C_\nu| = |D_\nu|$.

A. *Ansatz* (A)

We propose to consider this new *Ansatz*, in which both $|A_l| = |D_l|$ and $|A_\nu| = |D_\nu|$ hold. Our motivations are based on the model which we built in Sec. II:
(i) In the charged lepton sector, the (1,2) and (3,3) entries of the Yukawa coupling matrix Y_l^1 are nonzero. It is natural to assume that they have the same magnitude: $|(Y_l^1)_{12}| = |(Y_l^1)_{33}|$. After SSB, we arrive at $|(M_l)_{12}| = |(M_l)_{33}|$, or equivalently, $|A_l| = |D_l|$. In this assumption, we can reduce the number of free input parameters. This equality can be realized in the non-Abelian discrete group A_5 [24] with suitable arrangements of the particle contents[1]

---

[1]We may arrange ℓ_L and E_R as the triplets, H^1 as a singlet, and embed H^2 and H^3 to a 5-plet in A_5. After H^1 gains its vacuum expectation value, we are led to $A_l = D_l$. With a suitable vacuum alignment for the 5-plet, no additional mass term will be introduced and the two-zero texture is preserved.

(ii) Applying the above discussion to the neutrino sector, we are led to

$$|(M_D)_{12}| = |(M_D)_{33}|, \qquad |(M_S)_{12}| = |(M_S)_{33}|,$$

$$|(M_R)_{12}| = |(M_R)_{33}|, \qquad |(M_\mu)_{12}| = |(M_\mu)_{33}|. \tag{41}$$

Then, using the inverse seesaw formula in Eq. (9), we arrive at

$$|(M_\nu)_{12}| = |(M_\nu)_{33}|$$

$$= \frac{|(M_D)_{12}|^2|(M_\mu)_{12}|}{|(M_S)_{12}|^2 - |(M_\mu)_{12}||(M_R)_{12}|}, \tag{42}$$

or equivalently, $|A_\nu| = |D_\nu|$.

In *Ansatz* (A), the mass matrices in both the charged lepton and left-handed neutrino sectors can be solved exactly in terms of their mass eigenvalues. In the left-handed neutrino sector, we have the expression of $\bar{M}_\nu$ in terms of its three mass eigenvalues

$$|A_\nu| = (m_1 m_2 m_3)^{1/3},$$

$$|B_\nu| = [(m_1 m_2 m_3)^{1/3}(m_1 - m_2 + m_3) - 2(m_1 m_2 m_3)^{2/3}$$

$$+ m_1 m_2 - m_1 m_3 + m_2 m_3]^{1/2},$$

$$|C_\nu| = m_1 - m_2 + m_3 - (m_1 m_2 m_3)^{1/3}, \tag{43}$$

and that of U_ν in terms of the ratios of the eigenvalues

$$U_\nu = \begin{pmatrix} k_{\nu 1}(x_\nu y_\nu - a_\nu)a_\nu & k_{\nu 2}(y_\nu + a_\nu)a_\nu & k_{\nu 3}(1-a_\nu)a_\nu \\ k_{\nu 1}(x_\nu y_\nu - a_\nu)x_\nu y_\nu & -k_{\nu 2}(y_\nu + a_\nu)y_\nu & k_{\nu 3}(1-a_\nu) \\ k_{\nu 1}b_\nu x_\nu y_\nu & k_{\nu 2}b_\nu y_\nu & k_{\nu 3}b_\nu \end{pmatrix}, \tag{44}$$

where $a_\nu = |A_\nu|/m_3$, $b_\nu = |B_\nu|/m_3$, $c_\nu = |C_\nu|/m_3$ and

$$k_{\nu 1} = [(a_\nu^2 + x_\nu^2 y_\nu^2)(x_\nu y_\nu - a_\nu)^2 + x_\nu^2 y_\nu^2 b_\nu^2]^{-1/2},$$

$$k_{\nu 2} = [(a_\nu^2 + y_\nu^2)(y_\nu + a)^2 + y_\nu^2 b_\nu^2]^{-1/2}, \tag{45}$$

$$k_{\nu 3} = [(a_\nu^2 + 1)(1 - a_\nu)^2 + b_\nu^2]^{-1/2}.$$

In the charged lepton sector, after replacing the index $\nu \to l$ and the masses $(m_1, m_2, m_3) \to (m_e, m_\mu, m_\tau)$, we arrive at the expressions of $\bar{M}_l$ and U_l. The relations

$$\gamma_{e,1} = \gamma_{\mu,2} \pm 90° = \gamma_{\tau,3} \tag{46}$$

must be required in the phase matrices $P_{l,\nu}$, while $Q_{l,\nu}$ are arbitrary.

The mixing angles θ_{12}, θ_{23}, θ_{13} and the CP phases δ, ρ, σ can be obtained from $V \equiv V_l^\dagger V_\nu = P_l^\dagger U_l^\dagger \bar{Q} U_\nu P_\nu$.

The numerical results of the parameter space and phenomenological predictions in *Ansatz* (A) are shown in Fig. 3. Only three free parameters, m_1, α, and β, are taken
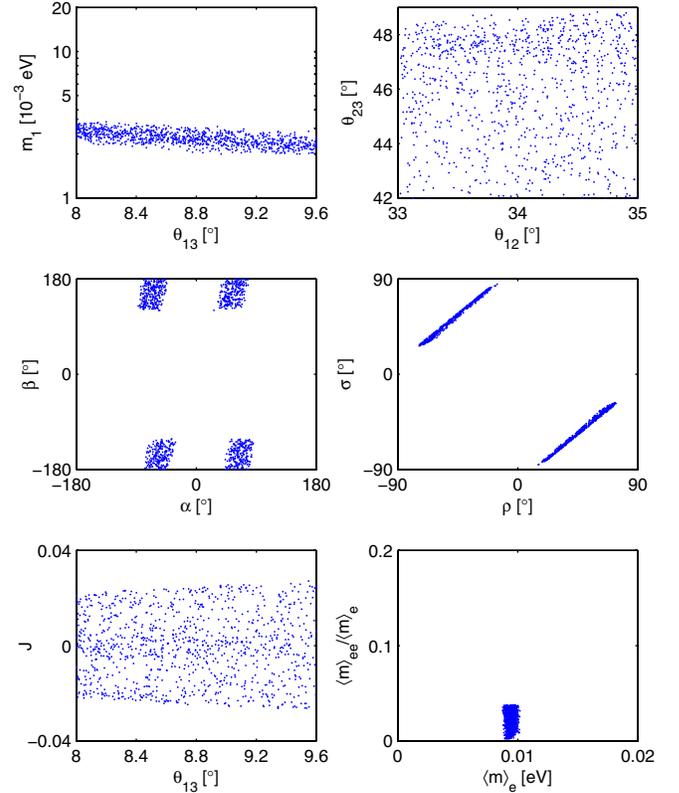
FIG. 3 (color online). The parameter space and phenomenological predictions of *Ansatz* (A). Only three free parameters α, β, and m_1 are adjustable. The constraints are the same as in Fig. 1.

as inputs. The experimental constraints are the same as those in the general case. The constraint on m_1 in this *Ansatz* is much stronger than that in the general case. One can get $m_1 \simeq (0.002–0.003)$ eV in Fig. 3. Although the number of free parameters has decreased to three, the numerical results of the mixing angles θ_{12}, θ_{23}, and θ_{13} still fit the experimental constraints very well. Among them, θ_{12} and θ_{13} are still nearly evenly distributed in the parameter space, and θ_{23} has a very slight preference for being larger than 45°. The CP-violating parameters are constrained more stringently. The allowed region of the (α, β) parameters is much smaller: $|\alpha| \simeq (45°–90°)$ and $|\beta| \simeq (120°–180°)$. $|\mathcal{J}|$ can maximally reach 0.02 at $\theta_{13} = 8°$ and 0.03 at $\theta_{13} = 9.6°$. The relation $\rho \approx \sigma \pm 90°$ is a good approximation. The ratio $\langle m \rangle_{ee}/\langle m \rangle_e$ is more likely to get a small value than that in the general case. It is only allowed in the range (0.002–0.04). Taking $\langle m \rangle_e \simeq 10^{-2}$ eV, we obtain $\langle m \rangle_{ee} \simeq (0.24) \times 10^{-4}$ eV. This is far beyond the sensitivity of the future experiments.

B. *Ansatz* (B)

In *Ansatz* (B), the requirements $|C_l| = |B_l|$ and $|C_\nu| = |D_\nu|$ are imposed. This *Ansatz* was first proposed in Ref. [8]. It is motivated by the mass hierarchy of the charged leptons and the experimental fact that the mixing angle θ_{23} in the MNSP matrix is about 45°. The relation

$|C_l| = |B_l|$ will lead to $|C_l| \approx |m_\mu|$, which is compatible with the fact that charged leptons have a large mass hierarchy. And the requirement $|C_\nu| = |D_\nu|$ can lead to $\theta_{23} = 45°$ easily. A detailed interpretation for this *Ansatz* can be found therein. Here, we reanalyze it by using the latest experimental data.

The solutions for diagonalizing M_l and M_ν in terms of the mass eigenvalues and their ratios have been give in Ref. [8]. We use them for our numerical calculation and show the relevant results in Fig. 4. The same inputs and constraints in *Ansatz* (A) are applied to this *Ansatz*. The lightest neutrino mass m_1 is given by $m_1 \simeq (0.004$–$0.008)$ eV, bigger than that in *Ansatz* (A). For the mixing angles $\theta_{13} > 8.8°$ and $\theta_{12} < 33.8°$ hold, and θ_{23} is easier to gain a value smaller than $45°$. As shown in Fig. 4, two thirds of the $(\theta_{12}, \theta_{23})$ parameter space is excluded. The constraint on the (α, β) parameter space is still loose, and the relation $\rho \approx \sigma \pm 90°$ is also valid. $|\mathcal{J}|$ in this *Ansatz* can maximally reach 0.02 at $\theta_{13} = 9.6°$, smaller than the maximal value in *Ansatz* (A). The prediction for the effective mass of the $0\nu2\beta$ decay is totally different from that in *Ansatz* (A). It gives $\langle m \rangle_{ee}/\langle m \rangle_e \simeq 0.1$. Since $\langle m \rangle_e \simeq 0.01$ eV also holds in this *Ansatz*, we arrive at $\langle m \rangle_{ee} \simeq 0.001$ eV. We can compare the new results with the old ones presented in Ref. [8]. Since the mixing

parameters are measured more precisely, most parts of the parameter space are excluded. *Ansatz* (B) now is not as favored as before.

In this section, we have analyzed the UTZT in two *Ansätze*. They have two main features distinguishing themselves from each other. One is the difference of the parameter space of the mixing angles. *Ansatz* (A) is favored in the full $(\theta_{12}, \theta_{23})$ parameter space, while *Ansatz* (B) is just partly favored. This feature makes *Ansatz* (A), which is a natural assumption of our model in Sec. II, more interesting than *Ansatz* (B). The other feature is the prediction for $\langle m \rangle_{ee}$. The value of $\langle m \rangle_{ee}$ in *Ansatz* (B) is much larger than that in *Ansatz* (A), although both are below the sensitivity of the near-future experiments.

VI. CONCLUSION

The GISM gives vanishing (1,1) and (1,3) submatrices of the 9×9 neutrino mass matrix $\mathcal{M}$. This is similar to the UTZT, which gives vanishing (1,1) and (1,3) elements of the 3×3 mass matrices $M_{l,\nu}$. We have pointed out their similarity and considered their several aspects. The main points are listed in the following:

(1) We have proposed a model based on the discrete Abelian group $Z_6 \times Z_6$ to realize both the GISM and the UTZT. We reiterate that besides Z_6, there are many discrete Abelian groups whose direct products can realize both of them.

(2) We have calculated the UTZT in the general case. Only the normal hierarchy of the neutrino masses is allowed by this texture. We obtain the lightest neutrino mass $m_1 \simeq (0.001$–$0.015)$ eV. The Jarlskog invariant $\mathcal{J}$ can maximally reach 0.04 in view of the new experimental results of θ_{13}. The effective mass $\langle m \rangle_{ee}$ in the $0\nu2\beta$ decay can maximally reach 0.001 eV.

(3) We have compared two *Ansätze* of the UTZT. *Ansatz* (A) is a natural approximation of our model built in Sec. II, and *Ansatz* (B) is a special case which has been considered in Ref. [8]. The mixing angles in *Ansatz* (A) fit the experimental constraints quite well, while in *Ansatz* (B), $\theta_{13} > 8.8°$ and $\theta_{12} < 33.8°$ are allowed, and $\theta_{23} < 45°$ is preferred. *Ansatz* (B) predicts the effective mass $\langle m \rangle_{ee} \simeq 0.001$ eV in the $0\nu2\beta$ decay experiments, while *Ansatz* (A) can only predict $\langle m \rangle_{ee}$ one or two orders of magnitude smaller than that in *Ansatz* (B).

Finally, we stress that the GISM can avoid the hierarchy problem and is testable in collider experiments, and the UTZT agrees very well with current neutrino oscillation data. Both the GISM and UTZT can be realized from the same Abelian symmetry due to their similar structures, although their uniqueness cannot easily be verified in the bottom-up approach of model building. Except for the above discussions, there are some other interesting aspects
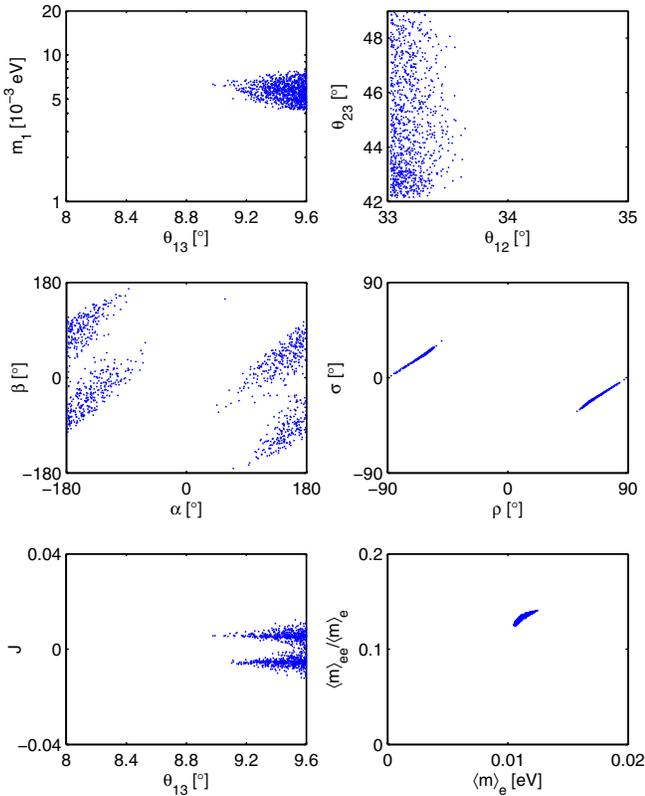
FIG. 4 (color online). The parameter space and phenomenological predictions of *Ansatz* (B). The inputs and constraints are the same as in Fig. 3.

of the GISM and UTZT in neutrino phenomenology. One is to discuss possible collider signatures of the TeV-scale right-handed, or additional gauge-singlet neutrinos in the GISM, which could be explored by the Large Hadron Collider. Another aspect is related to the baryogenesis via leptogenesis, so as to account for the cosmological matter-antimatter asymmetry. The two-zero textures of the Yukawa coupling matrices and the uncertainty of the scales of M_R and M_μ may affect how the leptogenesis mechanism works in the early Universe. A detailed analysis of these aspects will be done elsewhere.

ACKNOWLEDGMENTS

APPENDIX A: SIMPLIFICATION OF THE NEUTRINO MASS MATRIX IN THE GISM

1. General analysis

The neutrino mass matrix in the GISM is described by a 9×9 matrix $\mathcal{M}$ given in Eq. (2), where M_D, M_S, M_R, and M_μ are 3×3 complex submatrices. For physical conditions, one can naturally assume that the scale of M_D is the electroweak scale and the scale of M_S is several orders larger than that of M_D. To some extent, the scales of M_R and M_μ are more arbitrary. They can be either very high or very small due to different mechanisms. Large mass scales can be regarded as the breaking of a certain symmetry at a very high energy scale, similar to the Majorana mass matrix of the right-handed neutrinos in the type-I seesaw model. And small mass scales may be generated from higher-dimensional operators after integrating out some unknown heavy fields [25]. Small mass scales are also consistent with the 't Hooft's naturalness criterion [26], because the conservation of the lepton number is recovered when M_R and M_μ reduce to zeros.

Since different scales of M_R and M_μ may lead to different phenomenological consequences, it is necessary to do a general analysis of how $\mathcal{M}$ can be simplified in different cases. We denote

$$M_D' = (M_D \quad \mathbf{0}) \quad \text{and} \quad M_R' = \begin{pmatrix} M_R & M_S \\ M_S^T & M_\mu \end{pmatrix}. \quad \text{(A1)}$$

Obviously, the scale of M_D' is several orders smaller than that of M_S', and M_R' yields the masses of the right-handed and additional gauge-singlet neutrinos. One can obtain the mass matrix of light left-handed neutrinos through a seesawlike formula,

$$M_\nu \approx -M_D' M_R'^{-1} M_D'^T = -M_D (M_R - M_S M_\mu^{-1} M_S^T)^{-1} M_D^T. \quad \text{(A2)}$$

The mass formula in Eq. (A2) is the main result in the GISM. It can be further simplified in some special cases. However, since Eq. (A2) is only valid for $M_D \ll M_R - M_S M_\mu^{-1} M_S^T$, the exception should also be considered especially.

2. Special cases

For different mass scales of M_R and M_μ, the expression of M_ν in Eq. (A2) can be simplified. For the sake of convenience in the following dicussions, we denote M_R' to be block diagonalized by a 6×6 unitary matrix W as

$$W^\dagger M_R' W^* \equiv \begin{pmatrix} M_m & \mathbf{0} \\ \mathbf{0} & M_h \end{pmatrix}, \quad \text{(A3)}$$

in which M_m and M_h are 3×3 matrices standing for the medium and heaviest neutrino masses, respectively. Here, we consider three typical cases to simplify the mass matrices M_ν and M_R'.

Case (A): $0 \le M_R \ll M_S$ and $0 \le M_\mu \ll M_S$. Equation (A2) can be simplified to [27]

$$M_\nu \approx M_D M_S^{-T} M_\mu M_S^{-1} M_D^T, \quad \text{(A4)}$$

and M_R' is simplified to

$$M_R' \approx \begin{pmatrix} M_R & M_S \\ M_S^T & M_\mu \end{pmatrix}. \quad \text{(A5)}$$

This case has been discussed in Ref. [28]. Since M_μ and M_R are much smaller than M_S, the right-handed and additional gauge-singlet neutrinos have nearly degenerate masses and are combined to form the pseudo-Dirac particles. Their masses can be not huge and may be testable by the collider. For instance, assuming $M_\nu \sim 0.1$ eV, $M_\mu \sim 1$ keV, and $M_D \sim 10$ GeV, we obtain $M_S \sim 1$ TeV. Another aspect of this case is the nonunitary effects. Such effects in the mixing matrix are approximate to $M_D M_S^{-1}$. Experimental data show that they are smaller than $\mathcal{O}(1)$ [29]. Due to present accuracies for measuring mixing angles, we do not have to consider the nonunitary effects in the mixing matrix. We will ignore them in the main body of this paper.

Case (B): $M_\mu \ll M_S \ll M_R$. M_R' can be simplified to

$$M_m \approx M_\mu - M_S^T M_R^{-1} M_S,$$
$$M_h \approx M_R. \quad \text{(A6)}$$

This case accommodates a large range of the masses of sterile neutrinos and provides a possibility for low-scale leptogenesis [4]. One can further discuss the case (B1): $M_R \ll M_S M_\mu^{-1} M_S^T$ and case (B2): $M_R \gg M_S M_\mu^{-1} M_S^T$. In case (B1), M_ν can be simplified to Eq. (A4); while in case (B2), M_ν can be simplified to [4]

$$M_\nu \approx -M_D M_R^{-1} M_D^T. \qquad (A7)$$

To derive the tiny left-handed neutrino masses in case (B2), the scale of M_R should, in general, be very high, which is similar to the type-I seesaw model.

Case (C): $M_R \gg M_S$ and $M_\mu \gg M_S$. In this case we obtain Eq. (A7) and

$$M_m \approx \max(M_R, M_\mu),$$
$$M_h \approx \min(M_R, M_\mu). \qquad (A8)$$

The choice of the mass scale of M_μ is a little arbitrary except for $M_\mu \gg M_S$. There is only small mixing between the right-handed and additional gauge-singlet neutrinos.

Since Eqs. (A4) and (A7) are the typical formulas of left-handed neutrino mass matrices in the OISM and type-I seesaw model, respectively, these two models can be regarded as two special cases of the GISM to some extent.

3. Exception

Note that Eq. (A2) does not hold for $M_R - M_S M_\mu^{-1} M_S^T \lesssim M_D$. This exception should be considered in particular. It can be further divided into two cases: case (D), $M_R \lesssim M_D$ and $M_S M_\mu^{-1} M_S^T \lesssim M_D$; and case (E), $M_R \gg M_D$ and $M_S M_\mu^{-1} M_S^T \gg M_D$, but there is a cancellation that leads to $M_R - M_S M_\mu^{-1} M_S^T \lesssim M_D$.

Case (D): Since M_S is several orders higher than M_D, we are led to $M_R \ll M_S \ll M_\mu$. $\mathcal{M}$ can be simplified by a congruent transformation with a 9×9 unitary matrix $\mathcal{W}$. One can write out $\mathcal{W}$ and $\mathcal{W}^\dagger \mathcal{M} \mathcal{W}^*$ as

$$\mathcal{W} \approx \begin{pmatrix} 1 & 0 & 0 \\ 0 & 1 & -M_S M_\mu^{-1} \\ 0 & (M_S M_\mu^{-1})^\dagger & 1 \end{pmatrix},$$

$$\mathcal{W}^\dagger \mathcal{M} \mathcal{W}^* \approx \begin{pmatrix} 0 & M_D & 0 \\ M_D^T & M_R - M_S^T M_R^{-1} M_S & 0 \\ 0 & 0 & M_\mu \end{pmatrix}, \qquad (A9)$$

respectively. Finally, we obtain $M_\nu \approx M_D$, which is too heavy to be the left-handed neutrino mass matrix. Thus, this case is not interesting.

Case (E): $\mathcal{W}$ and $\mathcal{W}^\dagger \mathcal{M} \mathcal{W}^*$ are given by

$$\mathcal{W} \approx \begin{pmatrix} 1 & 0 & 0 \\ 0 & 1 & M_S^T M_\mu^{-1} \\ 0 & (M_S^T M_\mu^{-1})^\dagger & 1 \end{pmatrix},$$

$$\mathcal{W}^\dagger \mathcal{M} \mathcal{W}^* \approx \begin{pmatrix} 0 & 0 & M_D M_R^{-1} M_S \\ 0 & M_R & 0 \\ M_S^T M_R^{-1} M_D^T & 0 & 0 \end{pmatrix}, \qquad (A10)$$

respectively. One can further derive that the left-handed and additional gauge-singlet neutrinos have nearly degenerate masses $M_\nu \sim M_D M_R^{-1} M_S$ and form the pseudo-Dirac particles. However, since $M_S \gg M_D$, one has to require that the scale of M_R in the GISM be even higher than that in the type-I seesaw model, which is unnatural.

---

[1] P. Minkowski, Phys. Lett. **67B**, 421 (1977); T. Yanagida, in *Proceedings of the Workshop on Unified Theory and the Baryon Number of the Universe*, edited by O. Sawada and A. Sugamoto (KEK, Tsukuba, 1979), p. 95; M. Gell-Mann, P. Ramond, and R. Slansky, in *Supergravity*, edited by P. van Nieuwenhuizen, and D. Freedman (North Holland, Amsterdam, 1979), p. 315; S. L. Glashow, in *Quarks and Leptons*, edited by M. Lévy *et al.* (Plenum, New York, 1980), p. 707; R. N. Mohapatra and G. Senjanovic, Phys. Rev. Lett. **44**, 912 (1980).

[2] F. Vissani, Phys. Rev. D **57**, 7027 (1998); J. A. Casas, J. R. Espinosa, and I. Hidalgo, J. High Energy Phys. 11 (2004) 057; A. Abada, C. Biggio, F. Bonnet, M. B. Gavela, and T. Hambye, J. High Energy Phys. 12 (2007).061; Z. Z. Xing, Prog. Theor. Phys. Suppl. **180**, 112 (2009).

[3] D. Wyler and L. Wolfenstein, Nucl. Phys. **B218**, 205 (1983); R. N. Mohapatra, Phys. Rev. Lett. **56**, 561 (1986); R. N. Mohapatra and J. W. F. Valle, Phys. Rev. D **34**, 1642 (1986).

[4] S. K. Kang and C. S. Kim, Phys. Lett. B **646**, 248 (2007).

[5] M. Malinsky, T. Ohlsson, and H. Zhang, Phys. Rev. D **79**, 073009 (2009); M. Malinsky, T. Ohlsson, Z. Z. Xing, and H. Zhang, Phys. Lett. B **679**, 242 (2009).

[6] J. Ellis, J. L. Lopez, and D. V. Nanopoulos, Phys. Lett. B **292**, 189 (1992); J. Ellis, D. V. Nanopoulos, and K. Olive, Phys. Lett. B **300**, 121 (1993).

[7] P. H. Frampton, S. L. Glashow, and D. Marfatia, Phys. Lett. B **536**, 79 (2002); Z. Z. Xing, Phys. Lett. B **530**, 159 (2002); **539**, 85 (2002).

[8] Z. Z. Xing and H. Zhang, Phys. Lett. B **569**, 30 (2003).

[9] See, e.g., D. Du and Z. Z. Xing, Phys. Rev. D **48**, 2349 (1993); H. Fritzsch and Z. Z. Xing, Phys. Lett. B **353**, 114 (1995); K. Kang and S. K. Kang, Phys. Rev. D **56**, 1511 (1997); P. S. Gill and M. Gupta, Phys. Rev. D **56**, 3143 (1997); **57**, 3971 (1998); Nucl. Phys. **B556**, 49 (1999); G. C. Branco, D. Emmanuel-Costa, and R. G. Felipe, Phys. Lett. B **477**, 147 (2000); **506**, 109 (2001); R. Rosenfeld and J. L. Rosner, Phys. Lett. B **516**, 408 (2001); J. L. Chkareuli and C. D. Froggatt, Nucl. Phys. **B626**, 307 (2002); J. W. Mei and Z. Z. Xing, Phys. Rev. D **67**, 077301 (2003); H. Fritzsch and Z. Z. Xing, Phys. Lett. B

555, 63 (2003); Z. Z. Xing and H. Zhang, J. Phys. G **30**, 129 (2004).

[10] K. Kang, S. K. Kang, and U. Sarkar, Phys. Lett. B **486**, 391 (2000); W. L. Guo, Z. Z. Xing, and S. Zhou, Int. J. Mod. Phys. E **16**, 1 (2007); S. Rajpoot, arXiv:hep-ph/0703185; G. Ahuja, M. Gupta, M. Randhawa, and R. Verma, Phys. Rev. D **79**, 093006 (2009); J. Barranco, F. G. Canales, and A. Mondragon, Phys. Rev. D **82**, 073010 (2010); S. Dev, S. Kumar, S. Verma, S. Gupta, and R. R. Gautam, Eur. Phys. J. C **72**, 1940 (2012); J. Barranco, D. Delepine, and L. Lopez-Lozano, Phys. Rev. D **86**, 053012 (2012).

[11] L. J. Hu, S. Dulat, and A. Ablat, Eur. Phys. J. C **71**, 1772 (2011).

[12] W. Grimus, A. S. Joshipura, L. Lavoura, and M. Tanimoto, Eur. Phys. J. C **36**, 227 (2004).

[13] F. P. An *et al.* (Baya Bay Collaboration), Phys. Rev. Lett. **108**, 171803 (2012).

[14] J. K. Ahn *et al.* (RENO Collaboration), Phys. Rev. Lett. **108**, 191802 (2012).

[15] Z. Z. Xing, Chinese Phys. C **36**, 281 (2012).

[16] H. Fritzsch, Z. Z. Xing, and S. Zhou, J. High Energy Phys. 09 (2011) 083. This paper has studied seven kinds of two-zero textures systematically, and two types of them, A_1 and A_2, favor a relatively large θ_{13}, where A_2 is the same as M_ν in Eq. (3).

[17] H. Fritzsch and Z. Z. Xing, Prog. Part. Nucl. Phys. **45**, 1 (2000).

[18] L. E. Ibáñez and G. G. Ross, Phys. Lett. B **260**, 291 (1991); Nucl. Phys. **B368**, 3 (1992); **B398**, 301 (1993).

[19] J. Bergstrom, M. Malinsky, T. Ohlsson, and H. Zhang, Phys. Rev. D **81**, 116006 (2010).

[20] Z. Maki, M. Nakagawa, and S. Sakata, Prog. Theor. Phys. **28**, 870 (1962); B. Pontecorvo, Sov. Phys. JETP **26**, 984 (1968).

[21] Z. Z. Xing, H. Zhang, and S. Zhou, Phys. Rev. D **77**, 113016 (2008); **86**, 013013 (2012).

[22] C. Jarlskog, Phys. Rev. Lett. **55**, 1039 (1985).

[23] For a recent review, see S. M. Bilenky and C. Giunti, Mod. Phys. Lett. A **27**, 1230015 (2012).

[24] G. J. Ding, L. L. Everett, and A. J. Stuart, Nucl. Phys. **B857**, 219 (2012).

[25] E. Ma, Phys. Rev. D **80**, 013013 (2009).

[26] G. 't Hooft, in *Proceedings of 1979 Cargése Institute on Recent Developments in Gauge Theories*, edited by G. 't Hooft *et al.* (Plenum Press, New York, 1980), p. 135.

[27] M. K. Parida and A. Raychaudhuri, Phys. Rev. D **82**, 093017 (2010).

[28] E. Ma, Mod. Phys. Lett. A **24**, 2491 (2009).

[29] S. Antusch, C. Biggio, E. Fernández-Martínez, M. B. Gavela, and J. López-Pavón, J. High Energy Phys. 10 (2006) 084.